



**Proceedings
of the 4th Workshop
on the Medium-Energy
Electron Cooling**

JOINT INSTITUTE FOR NUCLEAR RESEARCH

MEEC'98

4th Workshop on the Medium Energy Electron Cooling

Proceedings

Editor: I. Meshkov

Dubna 1999

Contents

Foreword	5
MEEC WITH SINGLE PASS ELECTRON BEAM	
Electron Cooling of Hadrons in GeV Energy Range, <i>V. Parkhomchuk</i>	9
Prospectus for an Electron Cooling System for the Recycler, <i>A. Burov, C. Crawford, Th. Kroc, J. MacLachlan, S. Nagaitsev, Ch. Schmidt, A. Sharapa, A. Shemyakin, A. Warner</i>	25
Fermilab Conceptual Design for an Electron Cooler for 8 GeV Antiprotons, <i>J. MacLachlan</i>	113
Electron Beam Transport Scheme for the Fermilab Electron Cooling System, <i>S. Nagaitsev, A. Shemyakin</i>	129
Performance of Pelletron-based DC Recirculation System, <i>A. Crawford, S. Nagaitsev, A. Sharapa, A. Shemyakin</i>	144
Optimizing Parameters for Medium Energy Electron Cooling, <i>J. MacLachlan, A. Burov</i>	155
INJECTION & STORING SCHEMES WITH ELECTRON COOLING	
Colliders for Medium Energy with Electron Cooling, <i>A. Skrinsky, V. Parkhomchuk</i>	165
MEEC WITH CIRCULATING ELECTRON BEAM	
Particle Dynamics in the Sectional Modified Betatron, <i>I. Meshkov, A. Sidorin, A. Smirnov, E. Syresin</i>	167
Principle of Medium Energy Electron Cooling with Circulating Electron Beam, <i>I. Meshkov</i>	191
The Stability of the Circulating Electron Beam in the Electron Cooling System Based on the Modified Betatron, <i>A. Smirnov, I. Meshkov, A. Sidorin, E. Syresin</i>	198
Modified Betatron Prototype Dedicated to Electron Cooling with Circulating Electron Beam, <i>Yu. Korotaev, I. Meshkov, S. Mironov, A. Sidorin, A. Smirnov, E. Syresin</i>	212

RECENT DEVELOPMENTS IN ELECTRON COOLING

Analysis of First Measurements on SIS Electron Cooling of Heavy Ions, <i>V. Dolgashev, L. Groening, V. Parkhomchuk,</i> <i>A. Smirnov, M. Steck, T. Winkler</i>	229
Electron Cooling with a Bunched Electron Beam at the ESR, <i>T. Winkler</i>	244
Limitation of Ion Beam Intensity at Electron Cooling Systems, <i>V. Parkhomchuk</i>	254
Electron Cooling in COSY, <i>J. Stein, R. Maier, S. Martin, D. Prasuhn, J.D. Wiit</i>	258
New Technology for Control and Production of Precision Solenoids for Electron Cooling Systems, <i>A. Buble, N. Dikansky, V. Kudelainen,</i> <i>P. Lebedev, V. Parkhomchuk, B. Smirnov, N. Zubkov</i>	274
Plan for Electron Cooling R&D Facility at Wideband, <i>A. Warner</i>	285
Neutralized Electron Beam for Electron Cooling, <i>Yu. Korotaev, I. Meshkov,</i> <i>A. Petrov, A. Sidorin, A. Smirnov, E. Syresin,</i>	297

MEEC WITH SINGLE PASS ELECTRON BEAM

**Electron Cooling of Hadrons
in GeV Energy range**

V. Parkhomchuk

Electron Cooling of Hadrons in GeV Energy Range

HEACC'98, Dubna

V.Parkhomchuk, BINP (Novosibirsk)

1) first cooling NAP-M (Novosibirsk INP) (1974)

65 MeV (proton beam)

35 keV (electron beam)

ICE (CERN)

FNAL

LEAR, ESR, IUCF, CELSIUS, TSR ...

$1 \text{ MeV/n} \div 600 \text{ MeV/n}$

high energy projects

Electron Nucleon Collider (GSI)

Electron cooling for Recycler (FNAL)

Electron energy	5 MeV
Electron current	2 A
\bar{P} norm. emittance	$10 \pi \cdot \text{mm} \cdot \text{mrad}$
Beam radius	1.4 cm
$\Delta\Theta_{\perp}$	$7 \cdot 10^{-5} \text{ sec}$
τ cooling required	10^4 sec
n_e (at Lab. System)	10^8 1/cm^3
n'_e (at beam system)	10^7 1/cm^3

U_{238}^{90} - ELECTRON COLLIDER WITH ELECTRON COOLING

Ions kinetic energy GeV/u	9.18	27.5
Electron kinetic energy GeV	4	4
Circumference km	1	1
Ion weight A	238	238
Ion charge Z	90	90
Number of ions N_i	7.510^7	2.710^7
Number of electrons N_s	4.510^{10}	4.510^{10}
Emittance ε cm	3.810^{-7}	1.3610^{-7}
Bunch spacing D m	5	5
Beta IP β^* cm	10	10
Beta cooling β_{cool} m	100	100
Length on cooling section m	60	60
Part of cooling at orbit	0.06	0.06
Cooling current mA	6	4
Logarithm L_{cool}	5	5
Beam radius at cooling section cm	0.06	0.037
Beam radius at interaction point μm	19	11
ξ_i	0.05	0.05
ξ_e	0.05	0.05
luminosity ion-electron $cm^{-2}s^{-1}$	4.210^{30}	4.210^{30}
luminosity nukleon-electron $cm^{-2}s^{-1}$	10^{33}	10^{33}
Electron cooling kin energy MeV	5	15
Electron beam density (lab system) $1/cm^3$	5.310^7	910^7
Transverse momentum spread $\Delta p/p$	6.210^{-6}	3.710^{-6}
Transverse temper meV	1.1	3.2
cooling time sec	3.910^{-3}	910^{-2}

MOSOL 1980 – 1986

Ultimate possibilities of electron cooling

$H_{\max} = 4 \text{ kGs}$ $0.1\text{-}20 \text{ mA}$

$n_e = 2 \cdot 10^9 \text{ 1/cm}^3$ $\varnothing = 2\text{mm}$

$E_{\text{beam}} \text{ 450 – 500 eV}$

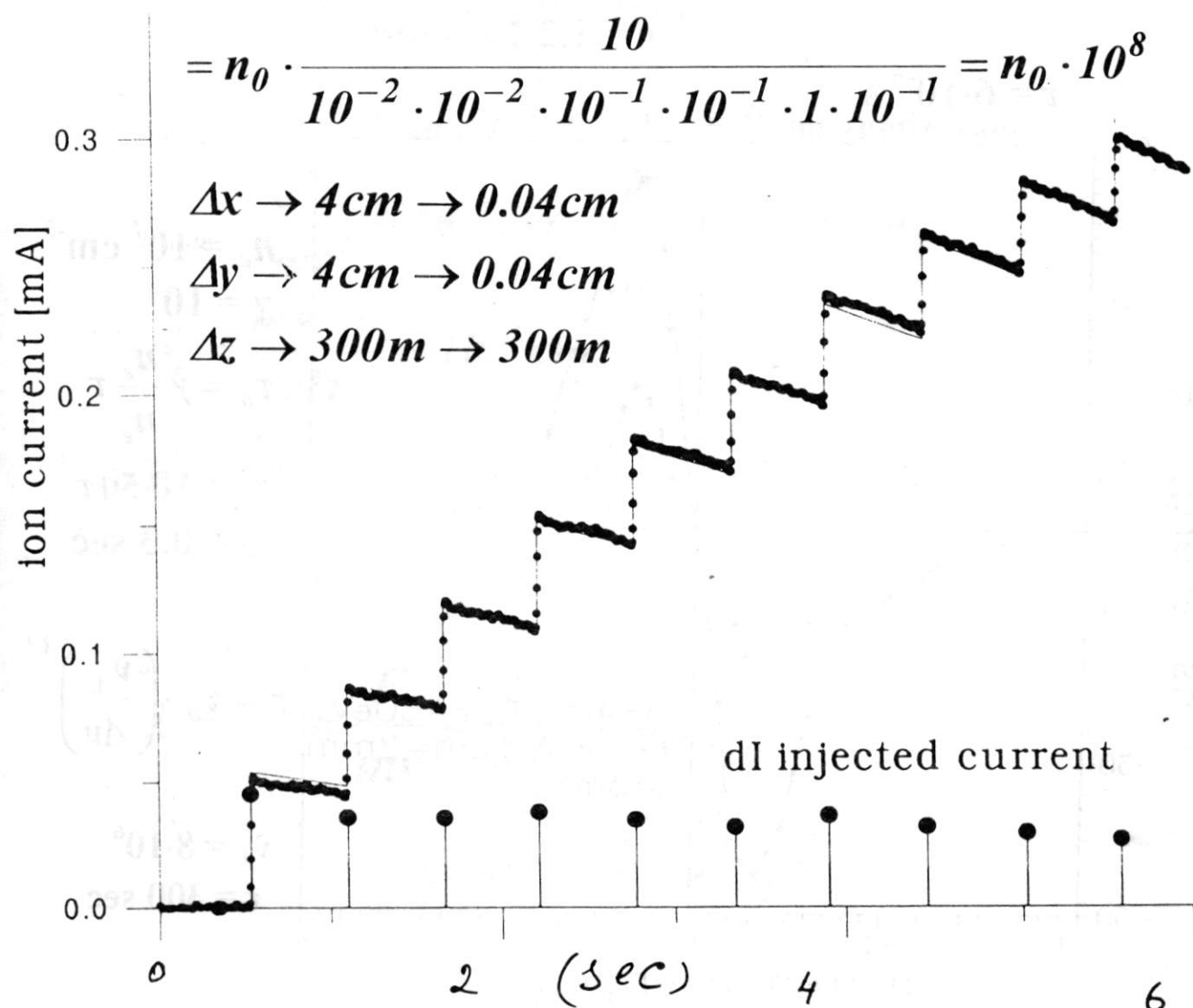
$$n = \frac{N}{\Delta x \cdot \Delta V_x \cdot \Delta y \cdot \Delta V_y \cdot \Delta z \cdot \Delta V_z} =$$

$$= n_0 \cdot \frac{10}{10^{-2} \cdot 10^{-2} \cdot 10^{-1} \cdot 10^{-1} \cdot 1 \cdot 10^{-1}} = n_0 \cdot 10^8$$

$\Delta x \rightarrow 4\text{cm} \rightarrow 0.04\text{cm}$

$\Delta y \rightarrow 4\text{cm} \rightarrow 0.04\text{cm}$

$\Delta z \rightarrow 300\text{m} \rightarrow 300\text{m}$



points - measurements

solid line - fit

Bi(+67)209, $J_e = 400 \text{ mA}$, exp. factor = 3

Cooling time

$$\frac{1}{\tau} = \frac{\vec{F}}{M\Delta\vec{v}} = \frac{v\Delta E_{loss}}{e\frac{M}{m}\Delta E_e}$$

$$n_e = 5 \cdot 10^8 \text{ 1/cm}^3$$

$$\Delta v = 0.8 \cdot 10^6 \text{ cm/s}$$

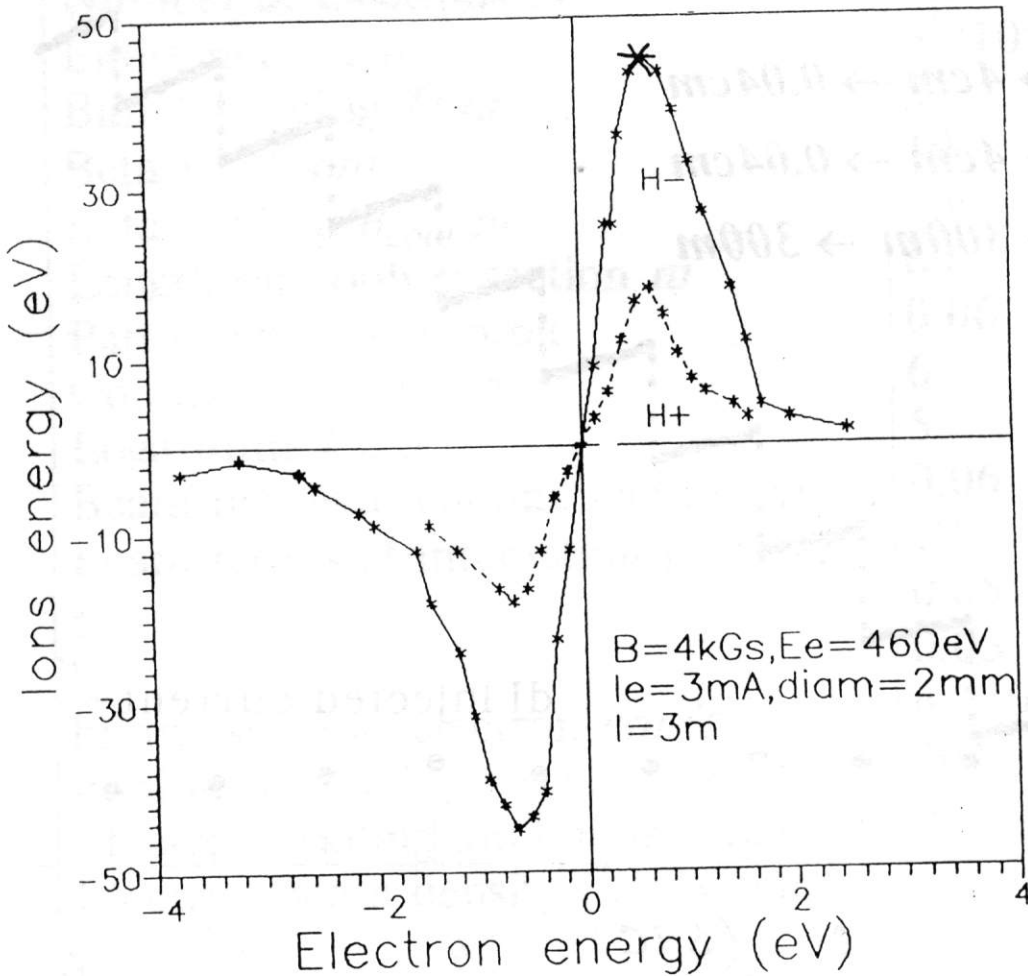
$$\Delta E_{loss} = 45 \text{ eV}$$

$$\Delta E_e = 0.6 \text{ eV}$$

$$\ell = 3 \text{ m}$$

$$v = 1.2 \cdot 10^9 \text{ cm/s}$$

$$\tau = 6 \cdot 10^{-6} \text{ s}$$



$$n_e = 10^7 \text{ cm}^{-3}$$

$$\gamma = 10$$

$$\tau_0 = \gamma \frac{n_e}{n_e} \tau$$

$$\tau_0 = 10 \cdot 50 \tau$$

$$\tau_0 = 0.3 \text{ sec}$$

$$\tau = \tau_0 \cdot \left(\frac{v_{\perp}}{\Delta v} \right)^3$$

$$v_{\perp} = 8 \cdot 10^6$$

$$\tau = 300 \text{ sec}$$

Friction force (at beam ref. system)

$$\vec{F} = -\frac{4e^4 n_e Z^2}{m} \cdot \frac{\vec{v}}{(v^2 + v_{eff}^2)^{3/2}} \ln \frac{(\rho_{max} + c_z \rho_{min} + \rho_L)}{(\rho_{min} + \rho_L)}$$

e – electron charge

n_e – electron beam density

\vec{v} - ion velocity

\vec{v}_{eff} - effective velocity electrons

$$\rho_{max} = v \cdot \tau \sim 1 \text{ cm}, \quad \rho > \rho_L, \quad v_{e\perp} \equiv 0 \quad \text{magnetization}$$

$$\rho_{min} = \frac{e^2 Z}{mv^2} \sim 10^{-5} \text{ cm}, \quad v_{eff} = \gamma v \cdot \Theta_{\perp}$$

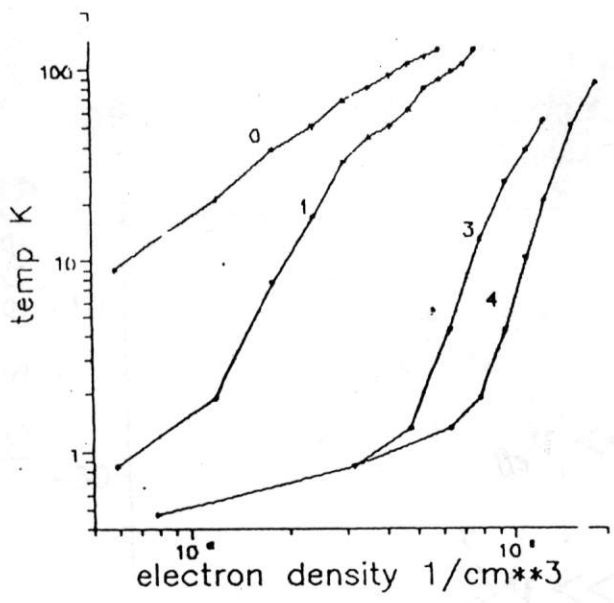
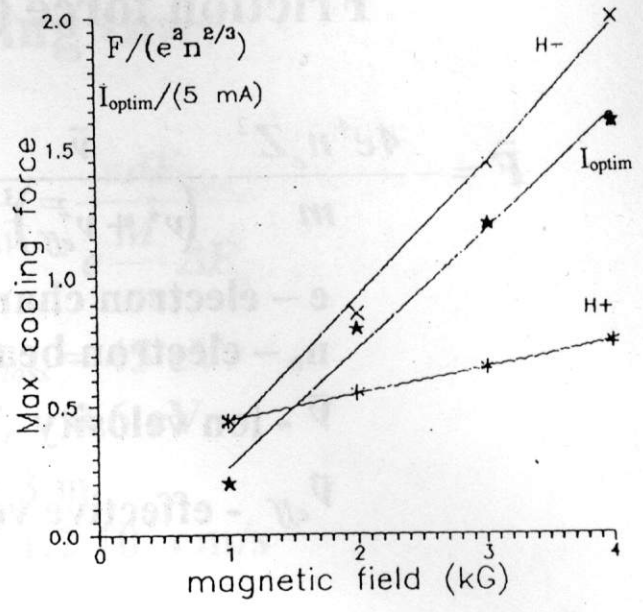
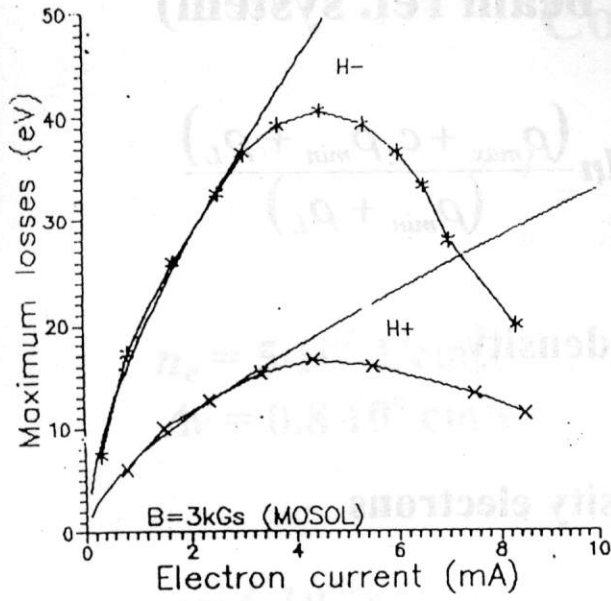
$$\rho_L = \frac{mV_{e\perp} c}{eH} \sim 10^{-3} \text{ cm}$$

$$F \sim \frac{1}{v^2} \quad v \gg v_{eff}$$

$$\sim v \quad v \ll v_{eff}$$

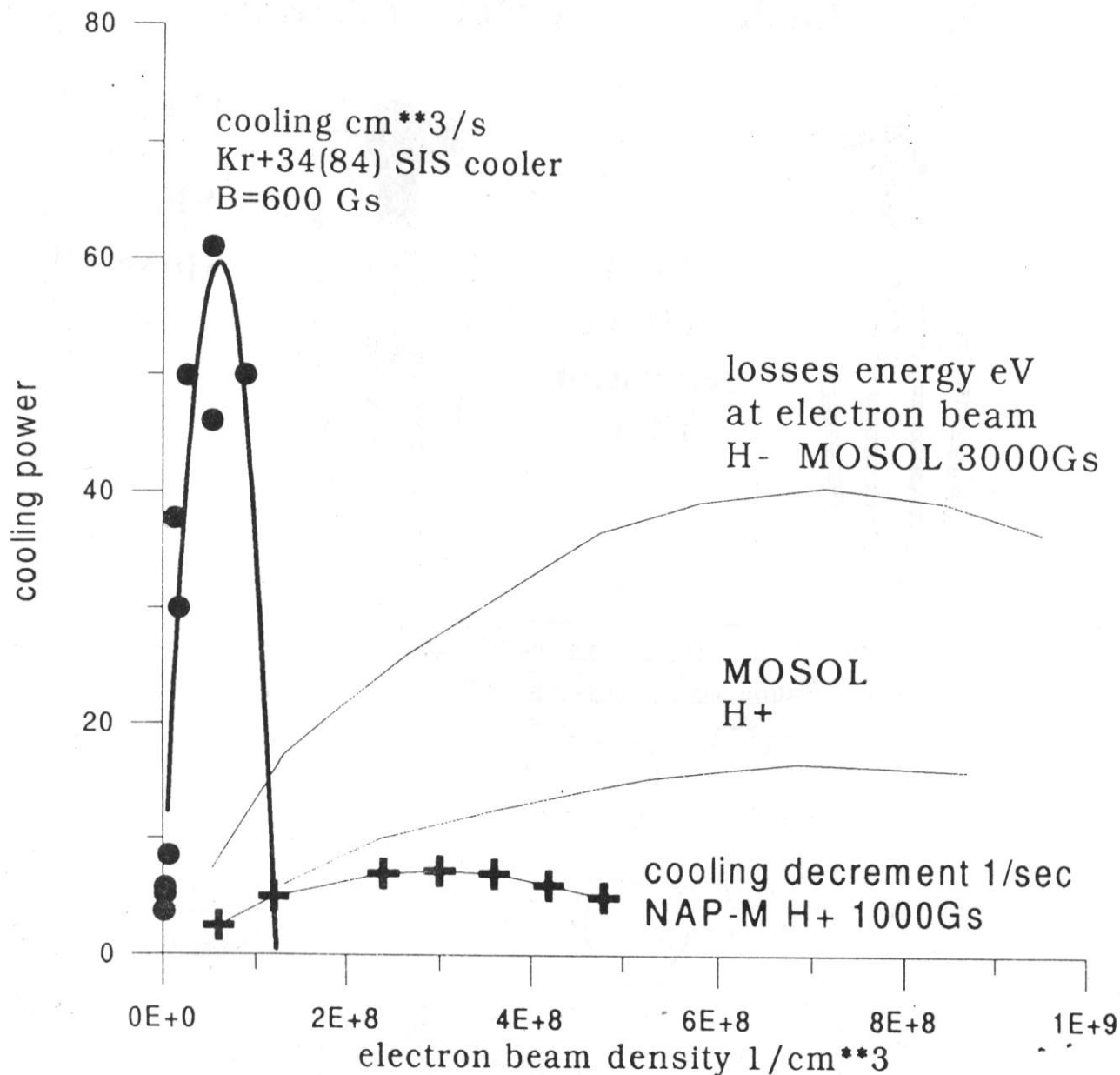
$$\lambda \approx \tau^{-1} \approx \frac{F}{mv} \approx \frac{1}{v^3}, \quad v \gg v_{eff}$$

$$\text{const} \quad v \gg v_{eff}$$



- 0 kGs – calculation
- 1 kGs
- 3 kGs
- 4 kGs

**Intra beam heating
at time single pass**



**For high field cooling saturation on
 more high electron beam density**

Novosibirsk

1 Mev \times 1 A (test)

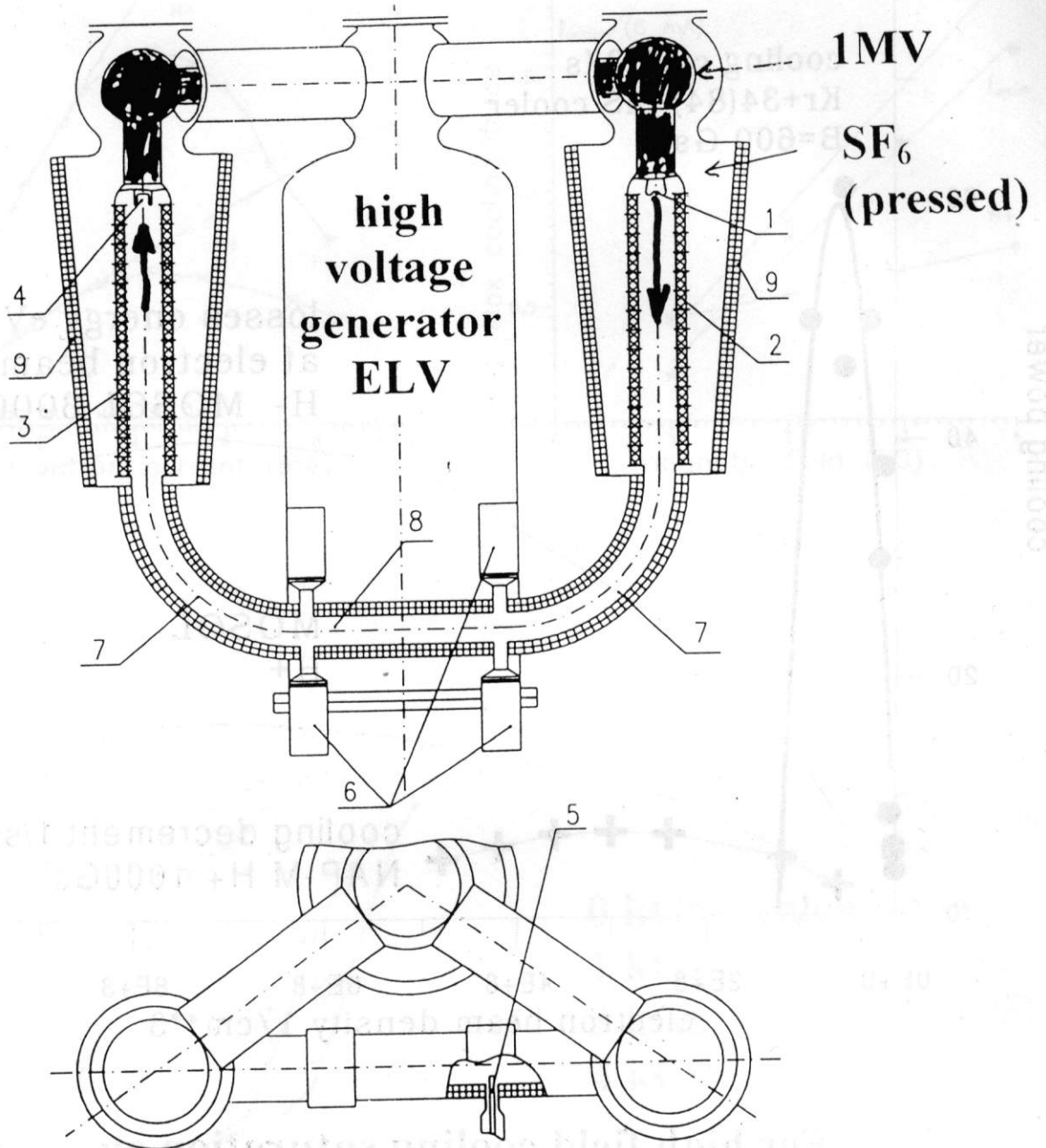


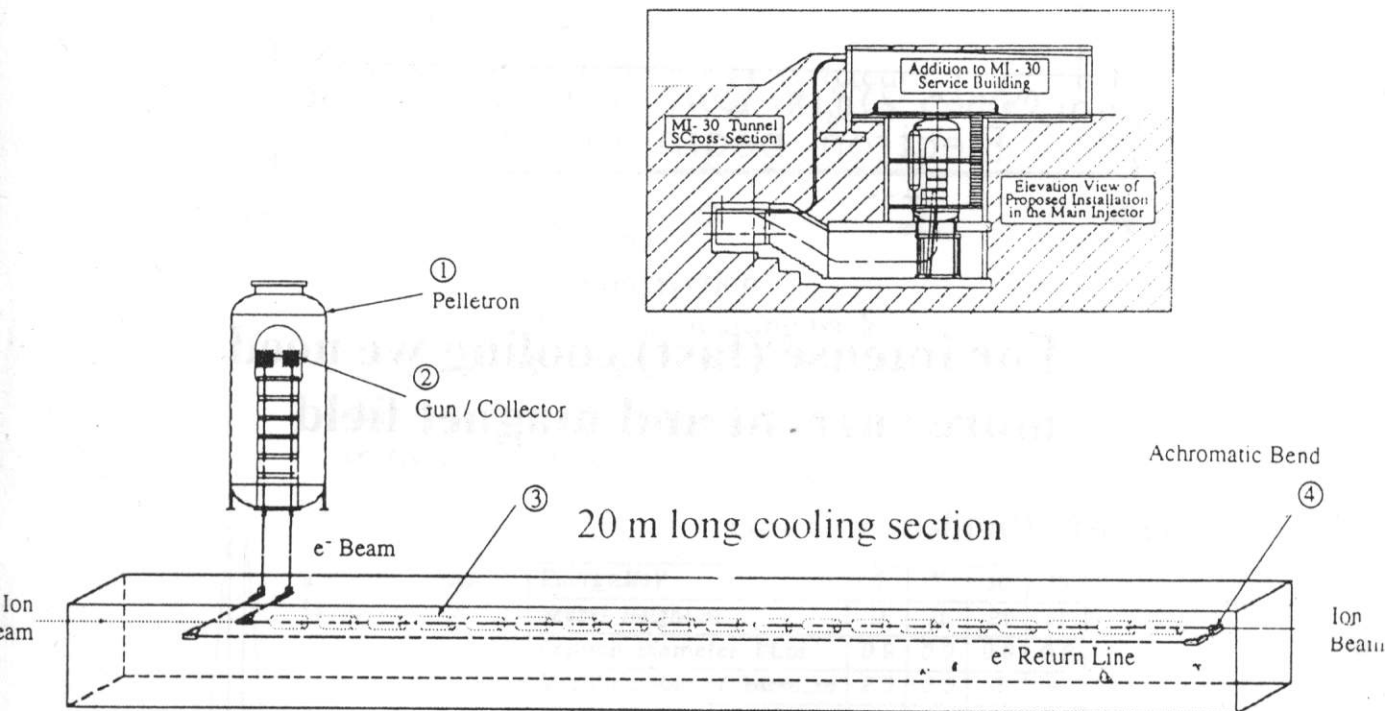
Figure 1: High voltage electron cooling device.

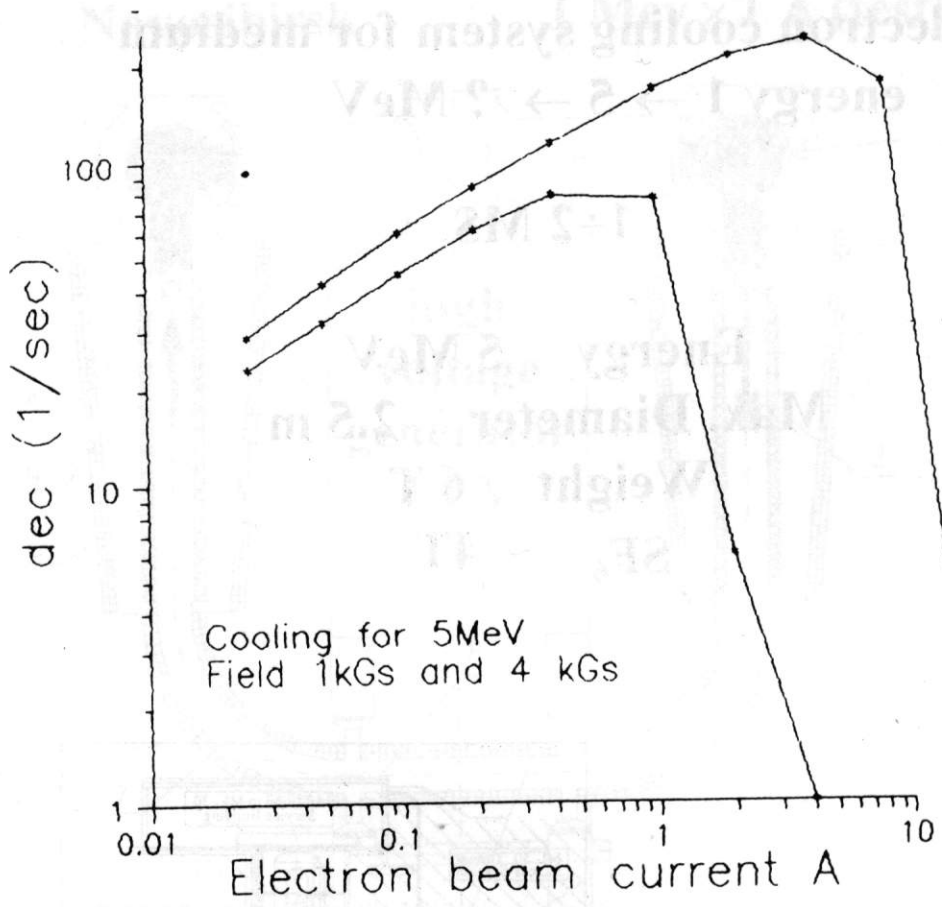
1 - cathod, 2, 3 - accelerating tubes, 4 - collector, 5 - reseiver, 6 - ion pumps, 7, 8, 9 - solenoids parts.

electron cooling system for medium energy 1 → 5 → ? MeV

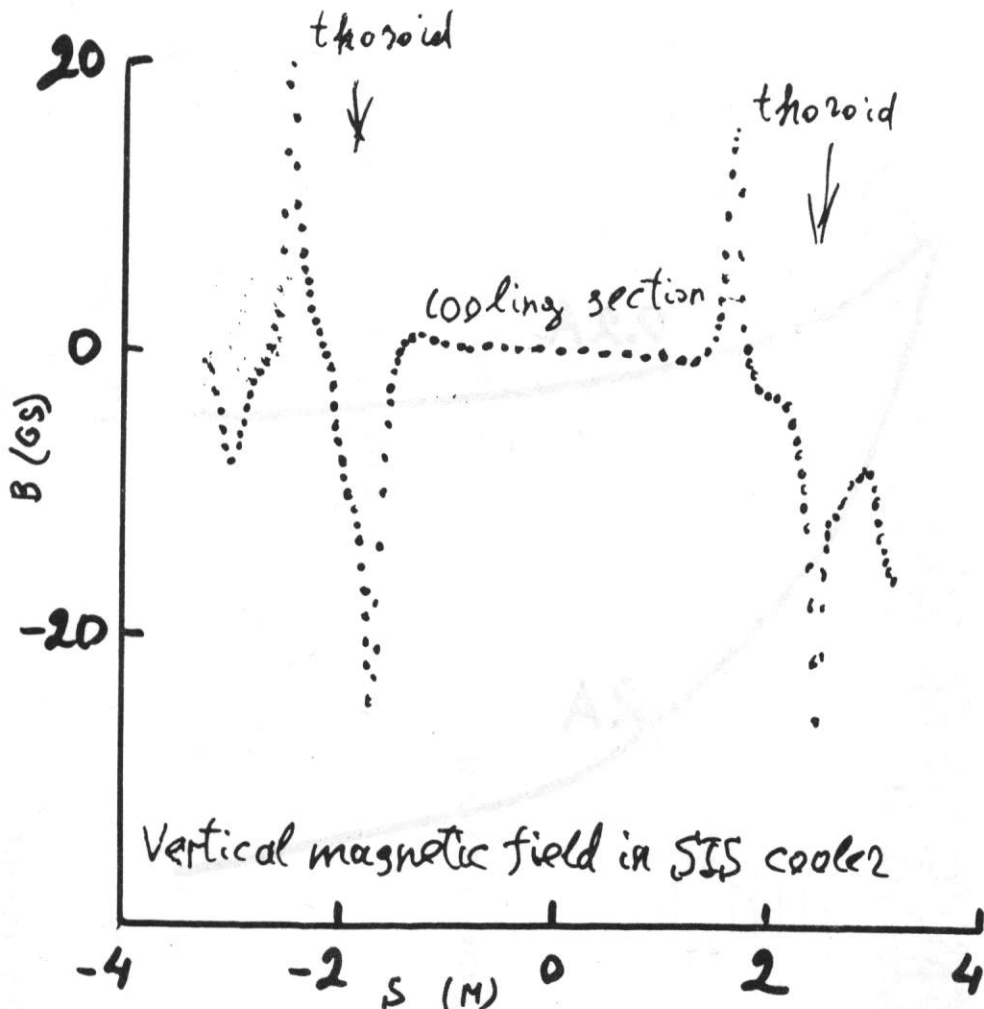
1 ÷ 2 MS

Energy 5 MeV
Max. Diameter 2.5 m
Weight 6 T
SF₆ ~ 4T



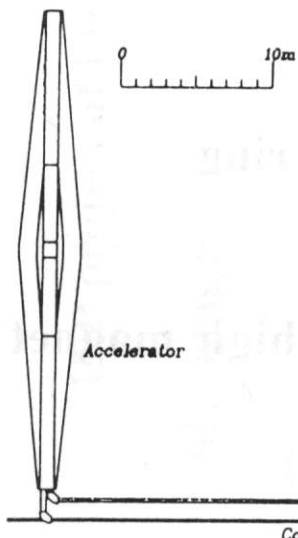


For intense (fast) cooling we need more current and magnet field



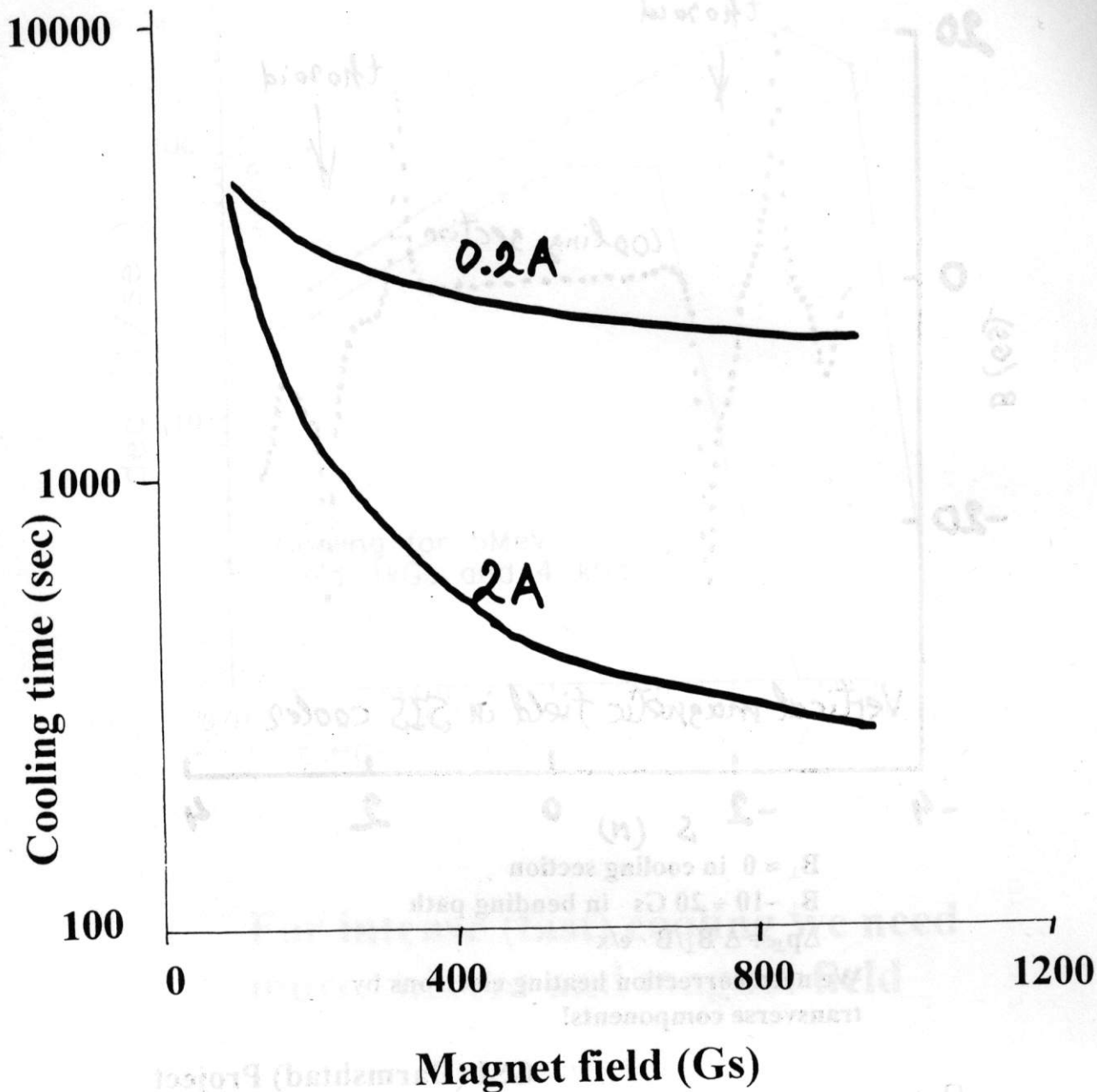
$B_{\perp} \approx 0$ in cooling section
 $B_{\perp} \sim 10 \div 20$ Gs in bending path
 $\Delta p_{\perp} = \Delta B_{\perp} / B \cdot e/x$
 We need correction heating electrons by transverse components!

GSI (Darmshtad) Project



Energy, MeV	5	7	10	15
Vessel Height, m	11	15	21	31
Column Diameter D1, m	0.9	0.9	0.9	0.9
Max Diameter of Vessel, m	2.5	2.5	3	4
Vessel Weight, T	6	7.5	17	38
Solenoids Weight, T	5	7	10	15
Vessel Volume, m ³	50	65	125	310
SF ₆ Weight, T	4	5.2	10	25
Power consumption, kW	65	90	130	200

Figure 6: The total view of cooling facility.



**Cooling for FNAL \bar{p} recycling ring
 \bar{p} amplitude 0.5 cm**

**If $I = 0.2$ A the profit from high magnet field
 not too large**

$\tau \sim 3000 \sim 4000$ sec ~ 1 hr (100 G)

$\tau \sim 300$ sec (1 kG) 2A

RF linac – based electron cooling device

98 MeV

$I_{av} \sim 50 \text{ mA}$

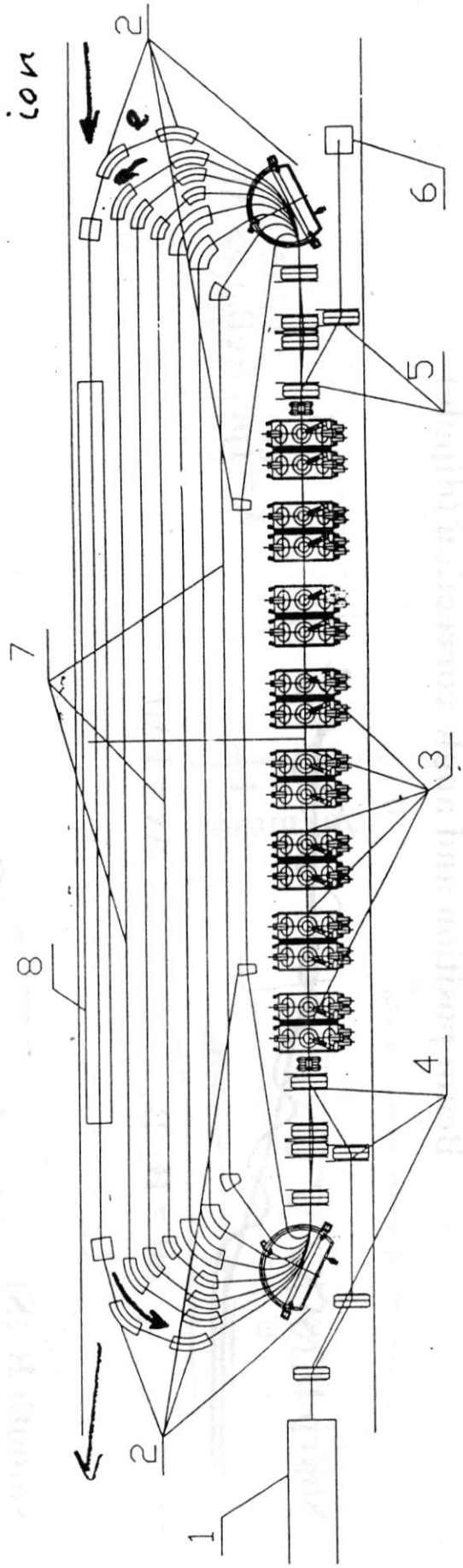
$I_{peak} \sim 10 \text{ mA}$

INP project of Free Electron Laser

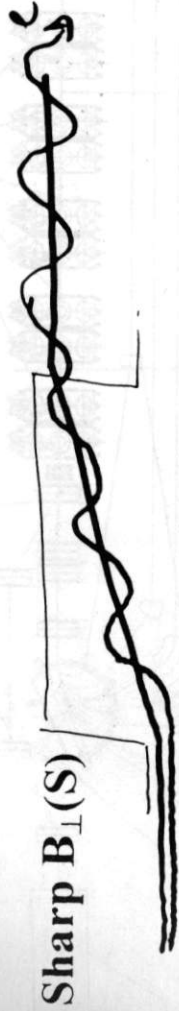
advantages:

- a) low electron beam
- b) very few orbit turns
- c) low average currents but large peak current

Good for bunch beam
cooling (ENC)



Beam position and angle correction (dipole)



$$\lambda = (pc) / (eB_0) \gg \Delta l$$

$$\Delta x = l \cdot \Delta \theta$$

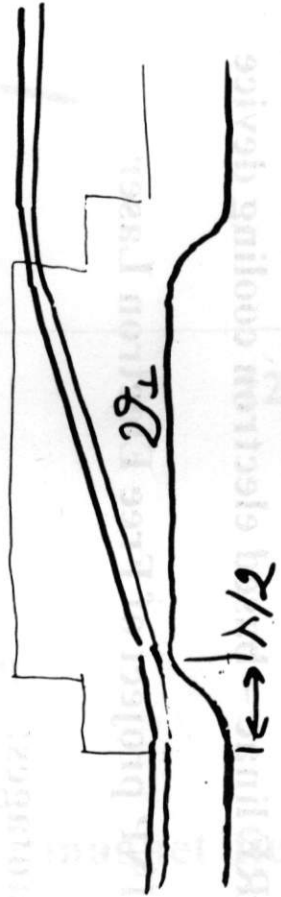
$$\Delta \theta = B_{\perp} / B_0$$

smooth $B_{\perp}(S)$



$$\lambda = (pc) / (eB_0) \ll \Delta l$$

resonance option



For high energy

$B_0 = 600 \text{ Gs}$

$E = 6 \text{ keV}$

$$\lambda = 0.42$$

$$\lambda = 2\pi\lambda = 2.6$$

$E = 5 \text{ MeV}$

$$\lambda = 27 \text{ cm}$$

$$\lambda = 170 \text{ cm}$$

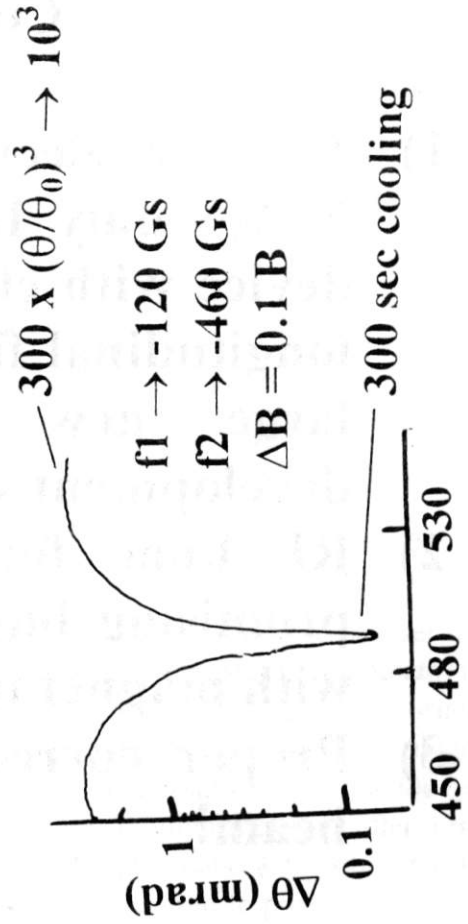
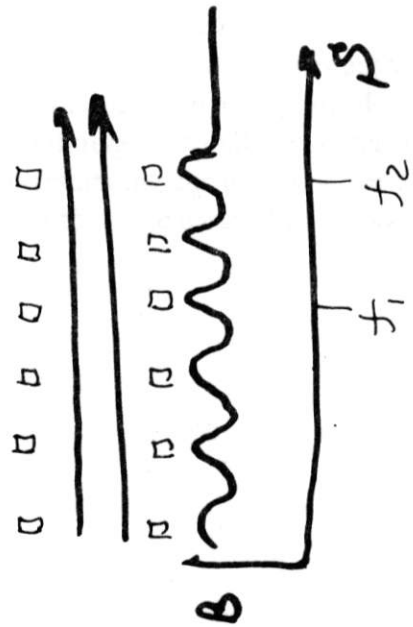
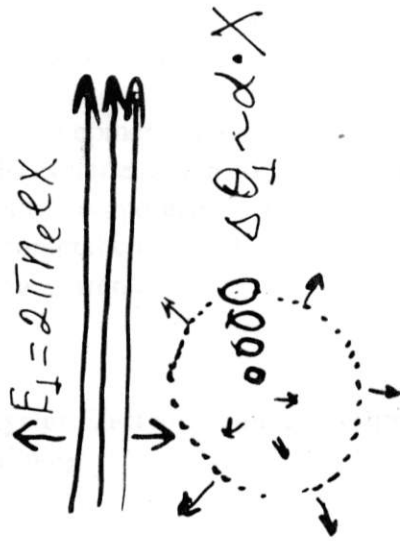
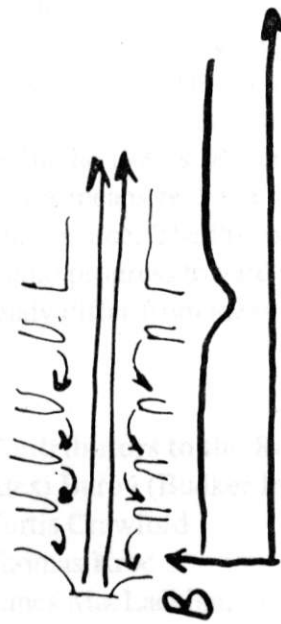
Focusing field corrections
(quadrupole components)

electrostatic fields of acceleration tube

Modulation magnet fields

Space charge fields inside
electron beam

Larmor transverse motion linear to X



Conclusion

- 1) For the electron beam energy range less 5 MeV only DC acceleration at electrostatic device with electron beam immersed in the longitudinal field can be used without very large new effort at research and development study.
- 2) RF linac for $E \gg 5$ MeV looks very promising but needs investigation of optics with magnet fields.
- 3) Proper correction system for the electron beam!

INJECTION & STORING SCHEMES WITH ELECTRON COOLING

Colliders for Medium Energy With Electron Cooling

A. Skrinsky, V. Parkhomchuk

Text is not presented

Limitation ion beam Intensity in electron cooling systems

V.V. Parkhomchuk, *Budker Institute of Nuclear Physics, Novosibirsk, 630090, Russia*

Abstract

Some effects making limitations for obtaining high ion currents are observed at interaction of an ion beam with an electron cooling beam. Dag Reistad pioneer of investigation these effects at CELSIUS called its electron heating. The same effect are limit of the proton beam intensity at the electron cooling ring at the Indiana University and many others storage ring. The last evidences of existing limitations was measurement at experiments with accumulation high Kr beam ion current in time of commission electron cooler in SIS (GSI) at May 1998. The nature of this limitation is not clear up to now but for future projects it can be very impotent factors. At this new projects the cooling of very intensive ions beam are used and we should be absolutely clear understand intensity limitations.

1 REVIEW OF EXPERIMENTAL RESULTS

1.1 Indiana University cooler

At the paper [1] we can read: "In the case of stripping injection, electron cooling system appears to be responsible for limiting the peak current in the ring to about 6 mA, this limit is more then an order magnitude below what we might expect without cooling". The cooler parameters: 0.3 A electron current, 2.5 cm beam diameter, 45 MeV proton energy, 2.5 m cooling section length, size of the cooled beam $a=0.1$ cm, momentum spread $\Delta p/p = 0.510^{-4}$ $\eta = 0.86$. The measurement was made for 1 mA current of RF-bunched proton beams with bunching factor of about 6 that correspond the coasting beams 6mA.

1.2 CELSIUS

At the CELSIUS facility [2] high losses in a beam were observed at proton currents from 4 to 25 mA, this is in correspondence with coasting currents without RF 25-300 mA (beam energy 48 MeV). The cooling of 50 mA electron beam with diameter 2 cm initial proton beam current from 25 mA drop down very fast and only 1-2 mA current have good life time as easy to see from Fig.2 in report [2].

An experiment on the helium ions cooling was carried out at the CELSIUS facility in December 1992. High losses were observed at 60 mA electron current as long as the ion current dropped below 0.04 mA. After that the ion losses sharply stopped and the beam life time became very long. They observed an injection under which only 0.02 mA was

injected in the ring as a result of an error in the injector, under this situation no losses at cooling were observed. This results reported [3] and in fig.4 (upper picture) shows a pickup signal when the current quickly decreases at 3mA injection, and one at 0.02mA injection when the signal slightly increases, this is connected with a decrease of the bunch length under cooling. Fig.4 (lower picture) clearly shows losses at repeated injections in the storage ring, and absolute absence of losses at a signal less than 41dB, this corresponds to 0.04 mA ion current. At the accelerating voltage switched off the beam extended over the whole orbit (coasting beam), and the threshold current increased to 0.52 mA, corresponding to a bunching factor about 13. When the electron current decreased to 30 mA, the ion current increased up to 1.6mA.

The experiments with accumulation the proton beam with energy 180 MeV was made at June-July 1997 and the accumulation process shows in figAcum. For this ex-

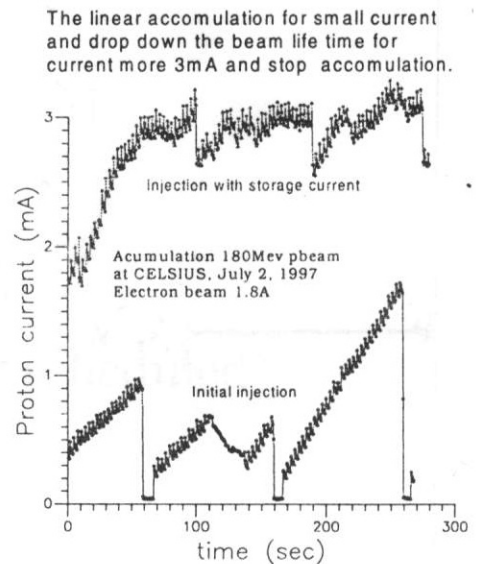


Figure 1: The accumulation 180 MeV proton beam, electron current 1.6 A (CELSIUS)

periments was founded that for small current it is not too large problems we have linear accumulation but if beam current was more 3-5 mA the beam losses becomes too large. The beam life time for current less them 2 mA was more 1000 sec but for 3 mA drop down to 160 sec and the proton beam losses limited the accumulation more beam current. The test of influences the electron beam energy

modulation was made at this experiments. The modulation of the electron beam energy increase the momentum spread at the storage ion beam. The fig. 2 demonstrates the accumulation near maximum ion current with the energy modulation and without. The modulation improved the lifetime the proton beam from 190 sec to 390 sec but by decreasing the cooling we not increase maximum current. The new results CELSIUS about positive action the

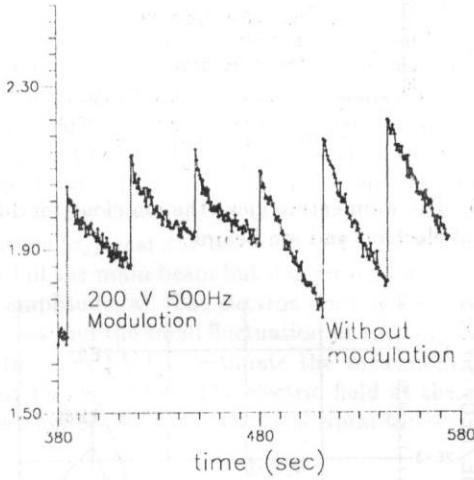


Figure 2: The influence the electron beam energy modulation 180MeV,0.3A (CELSIUS)

electron energy modulation reported at EPAC-98 [4]

1.3 SIS cooler

The last one result about same limitation on maximal cooling ion current was obtain at time of commission electron cooler for SIS (GSI) [5]. At fig 3 shown the signal the ion beam current and the signal of pickup electrodes at time of experiments for accumulation maximal ion current. At initial moment we have almost linear accumulation but after storage ion beam current 2 mA we see increasing same oscillation at ion beam and accumulation drop down and near 5 mA we see the saturation of process accumulation.

1.4 Equilibrium at the cooled beam core

The many experiments with cooling intensive ion beam indicated that the ion beam density limited so called Laslet tune shift the betatron oscillation. The value of Laslet tune shift is equal to:

$$\Delta\nu = \frac{Nr_i\beta_r R}{2a^2l_b\beta^2\gamma^3}, \quad (1)$$

where β_r is an beta function. The measuring for many cooler ring show that usually for intensive beam value of tune shift is equal $\Delta\nu = 0.2 - 0.4$.

The parameters of beams (E_e -electron beam energy, I_e -electron beam current, I_i - maximal ion beam peak

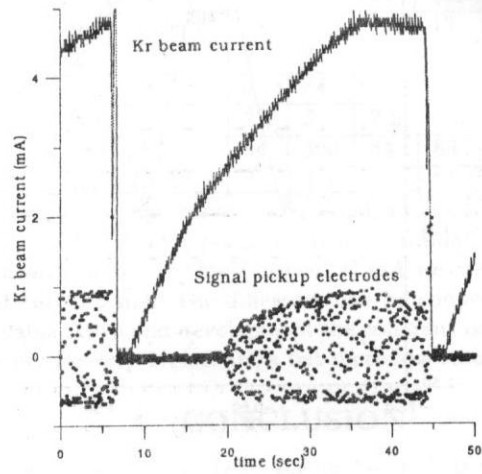


Figure 3: The accumulation Kr(84)(+34) beam at SIS 11.4MeV/n,0.8A,expf=3

current, a -ion beam radius, n_e -electron beam density, n_i -ion beam density) for this model shows in table 1.

E_e (keV)	6	6	25	100
I_e (A)	.06	0.2	0.3	1
Z	2	34	1	1
A	4	84	1	1
I_i (mA)	0.5	5	6	5
a (mm)	.6	4	1	0.3
$n_e/10^{11}/cm^3$	1.6	5.6	4.2	12
$n_i/10^{11}/cm^3$	2.7	0.038	12	60

2 MODEL FOR ESTIMATION INSTABILITY

Let me for the explanations of nature of this limitation calculate losses of the energy at ion beam after passing the cooling section the some fluctuation inside ion beam [6]. For example take the spherical region at the ion beam with displacement x and the velocity of motion v . The electric field at ion plasma generated this fluctuation is equal: $E = 4\pi n_i e x$, where n_i -density of ion beam, e -charge of ion. In a case moving fluctuation section displacements ions at time of flight the cooling section (τ) is equal $x = v\tau$. As the result of the action this field the electrons will shift from the equilibrium position on distance equal to: $\Delta x_e \sim \frac{eE}{m} \tau^2 = \frac{4\pi e^2 n_i \tau^3}{m} v$ and this disturbance of the electron flow generate the electric field: $E_e \sim 4\pi n_e \Delta x_e = \frac{(4\pi)^2 e^3 n_i n_e \tau^3}{m} v$ where n_e -density of the electron beam. This field produce the transverses kick at the ions near the region of fluctuation equal to:

$$\delta p = -A \frac{(4\pi)^2 e^4 n_i n_e \tau^4}{mM} Mv = -A\lambda p, \quad (2)$$

where p -ion momentum, M -ion mass, A -numerical coefficient which can be calculated by the careful integration of the motion equation at time of interaction. The parameter

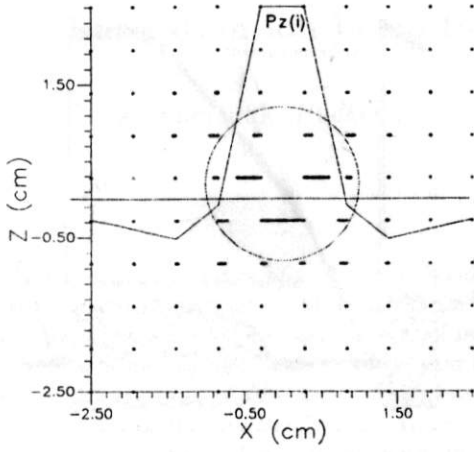


Figure 4: The section of ion beam after passing cooling section. The circular show region of fluctuation, the points the position of electrons, the line distribution of the transverse momentum by action of electric field.

λ is useful for estimation of interaction between the ions and the electron beam:

$$\lambda = (4\pi)^2 e^4 n_e n_i r_e r_i (c\tau)^4 = \omega_e^2 \omega_i^2 \tau^4 \quad (3)$$

where $r_e = e^2/mc^2$, $r_i = e^2/Mc^2$ -the electron and ion classical radii, ω_e , ω_i -the electron beam and ion beam plasma frequencies. On the fig. 2 model for the computer simulation with using the quasiparticles method is showed. The electric fields are calculated as differences between not movably background particles with a negative charge and moving particles. The quasiparticles were taken as spheres with a radius equal to half distance of grating. The fig. 5 shows the momentum kicks $\delta p/p_{x,v}$ and sum of squares of the momentum $\sum (\delta p/p_{x,v})^2$, where the normalized momentum is equal $p_v = vM_s$, $p_x = x/\tau M_s$, $M_s = M4\pi a^3/3 * n_i$ -mass of coherent fluctuation. The momentum kick increases with the electron beam density up to density where the $\omega_e > 1/\tau$ and the time of interaction is limited by Debay screening. The numerical fitting of the result (for magnetization electron with small temperature) shows that the momentum kick can be write as:

$$\delta p = -2 \cdot 10^{-3} \lambda M v - 5 \cdot 10^{-3} \lambda M \frac{x}{\tau} \quad (4)$$

and the energy losses after passing the electron beam equal:

$$\frac{\Delta E}{E} = -2 \cdot 10^{-3} \lambda + 10^{-5} \lambda^2 + 10^{-4} \lambda^2 \left(\frac{\beta}{l}\right)^2 \quad (5)$$

In this equation it is taken into account that for the amplitudes of fluctuation at the cooling section a relations $\langle x^2 \rangle = \langle v^2 \rangle / (v0\gamma)^2 * \beta_x^2$ and $\langle x * v \rangle = 0$ exist. Fig. 6 show the variation of $\Delta E/E/\lambda$ for different density the ion and electron beams. As easy see for the too high ion density cooling becomes heating (for $\tau = 10^{-8}$.

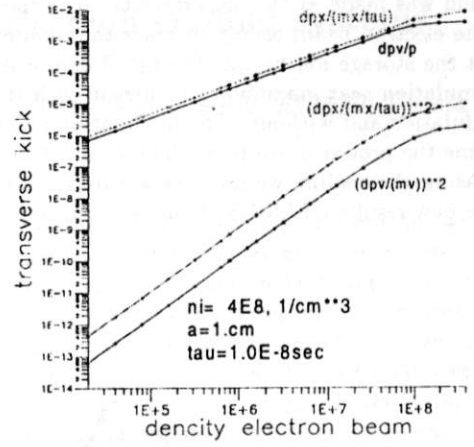


Figure 5: The momentum kicks the ion cloud for different density of electron and ion beams.

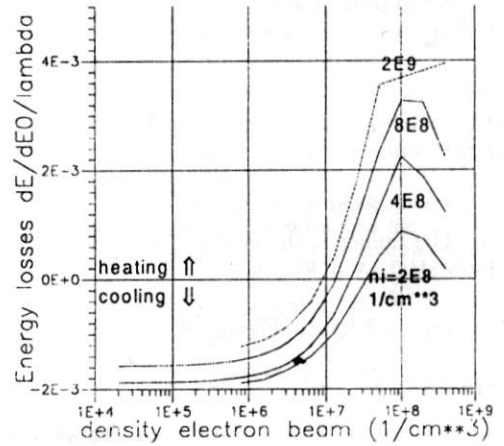


Figure 6: The losses energy of ion beam after passing cooling section: if loses negative it means cooling,if positive it means heating.

From equation 5 we can estimate the threshold value of parameters λ_{th} as:

$$\lambda_{th} = \frac{20}{0.1 + (\beta_{x,z}/l)^2} \quad (6)$$

The parameters λ is limited by the interaction ions inside beam (Laslet tune shift) and Debay screening inside electron beam. From results of computer simulation we can write estimation as $\lambda = (\omega_e \tau)^2 \Delta \nu_L \nu^2 (2\pi\eta) * 2/(1.0 + (\omega_e \tau)^2/40)$, where ν and $\Delta \nu_L$ - tune and Laslet tune shift, η -fraction cooling at beam orbit. For the standard parameters $\lambda_{max} \sim 2 - 10$. For the correct choice $\beta_x \sim l$ from equation 6 it is easy to see that the phenomenon of electron heating is not work $\lambda_{max} < \lambda_{th}$ but if $\beta_x \gg l$ the heating can limited the ion beam intensity. For experimental results from table 1 easy to calculate the value of λ as shows at table 2.

Ee (keV)	6	6	25	100
$n_e/10^{17}1/cm^3$	1.6	5.6	4.2	12
$n_i/10^{17}1/cm^3$	2.7	0.038	12	60
l_c (m)	2.5	3	2.5	2.5
τ nsec	54	65	26	12
λ	20	28	13	10

As easy to see the maximal value of λ 10-20.

3 THE LIMITATION OF THE BEAM CURRENT ACCUMULATION

As you can see the interaction the ion beam with electron beam made same-limitation on the ion beam density. It is very interesting how to calculate the limitation on the current. When we accumulate the large ion current the ion beam density limited the Laslet tune shift and not increase not too much. If at the core beam with the very small beam size are development the coherent oscillation with amplitude (a_c) near the beam size. This small oscillation is not kill the main beam but dangerous for the ions with large amplitude (a). The electron cooling for this ions are very weak and the small fluctuation at the core beam easy heat this ions. Let to estimate the maximum ion beam current for this effect. The electric field at the system of the rest ion beam at this model is equal to:

$$E_{\perp} = \frac{2eZN}{a^2 l_b \gamma} a_c \quad (7)$$

where l_b -length of the ion bunch, N-number of ions at bunch. The frequency bandwidth of this oscillation is $\Delta\omega = n\omega_0\eta_t \Delta p/p\gamma$. The heating of the transverse motion ion we can write as:

$$\frac{dp^2}{dt} = \frac{(eZE_{\perp})^2}{\Delta\omega} \quad (8)$$

The power electron cooling can be written as:

$$\frac{dE}{dt} = -\frac{4\pi\epsilon^4 Z^2 n_e \eta Lnc}{m(a/\beta_c)c\beta\gamma^2} \quad (9)$$

where n_e -density of electron beam at lab. system, η -fraction of the cooling section at the beam orbit, Lnc -Coulomb logarithm, β_c -beta function at cooler. The condition cooling looks as:

$$\frac{dp^2}{dtM} + \frac{dE}{dt} < 0. \quad (10)$$

For estimation we take value $a_c = a_L$ where a_L equilibrium beam size limited maximal value the Laslet tune shift $\Delta\nu$. The maximal harmonic number estimate as $n = 2\pi R/a$. All this condition can be write at form for the maximal cooled ion beam peak current:

$$I_{peak} = eZc\beta \left(-\frac{2\pi M Lnc n_e a^2 \eta \eta_t dp/p\gamma^4 \beta^2}{mZ^2 r_i R} \right)^{1/3} \quad (11)$$

For the experimental results discussed at table 1 this equation gives maximal ion currents shows at table 3 at assumption that $\Delta p/p = 10^{-4}$

Ee (keV)	6	6	25	100
$n_e/10^{17}1/cm^3$	1.6	5.6	4.2	12
Z	2	34	1	1
A	4	84	1	1
l_c (m)	2.5	3	2.5	2.5
$2\pi R$ (m)	84	300	84	84
I_{peak} (mA)	2	4.5	4.6	21

As easy to see agreement looks good and only for high energy (100 keV) at experiment with accumulation proton beam with energy 180 MeV instead 21 mA we can accumulated only 5-6 mA. The difference can be connected with less value $\Delta p/p$ and development the coherent oscillations not only for very high $n=R/a$ but more low resonances.

4 CONCLUSION

The electron cooling increase the ion beam density at 6 dimensional phase space at many order of magnitude. But so extremely cooled ion beam have problems with development coherent oscillation. The experimental results show that at many case the electron beam are responsible for this oscillation. And if the proposals of this report are close to reality the optimal length of cooler should be careful study for the new project of cooler. I am very grateful to Dag Reistad for interesting discussion about electron heating phenomena.

5 REFERENCES

- [1] Anderson D., Ball M., Derenchuk V., East G., Ellison M., Ellison T., Friesel D., Hamilton B.J., Nagaitsev S.S., Sloan T., Schwandt P., Cooled beam intensity limits in the IUCF cooler, Proc. Workshop on Beam Cooling and Related Topics, Montreux, Switzerland 4-8 Oct.1993, CERN 94-03, 26 April 1994 PS Division, pp.377-381.
- [2] Reistad D., Hermansson L., Bergmark T., Johansson O., Simonsson A., Burov A.V. Measuring of electron cooling and "electron heating" at CELSIUS, Proc. Workshop on Beam Cooling and Related Topics, Montreux, Switzerland 4-8 Oct.1993, CERN 94-03, 26 April 1994 PS Division, pp.183-187.
- [3] Parkhomchuk V.V., "Limitation beam intensity at electron cooling" Workshop on the Medium Energy Electron Cooling, 1997, pp. 11-18, Novosibirsk.
- [4] M.Bengtsson, T. Bergmark, H. Calen, ... , "New developments at CELSIUS" EPAC-98, Stockholm, p.514-515.
- [5] M.Steck, K.Blashe, W.Bourgeois, B.Franzke, ..., p.1185, EPAC 1996, Sitges, Spain
M.Steck, K.Blashe, H.Eickhoff, ..., "Commissioning of the electron cooling device in the heavy ion synchrotron SIS", EPAC 1998, Stockholm.
- [6] Parkhomchuk V.V., Pestrikov D.V., Coherent instabilities at electron cooling, Proc. Workshop on Beam Cooling and Related Topics, Montreux, Switzerland 4-8 Oct.1993, CERN 94-03, 26 April 1994 PS Division, pp.327-329.

New technology for production of precision solenoid for electron cooling systems

A.V.Bublei, N.S.Dikansky, V.I.Kudelainen, P.K.Lebedev,
V.V.Parkhomchuk, B.M.Smirnov, N.I.Zubkov
Budker Institute of Nuclear Physics, Novosibirsk

Abstract

An electron cooler was built at the Budker INP for the heavy ions synchrotron SIS at GSI, Darmstadt. A precision solenoid, 0.4 m in the inner diameter and over 3 m long with a magnetic field uniformity of about 10^{-5} makes the main part of the cooler. The paper describes in detail the solenoid production and techniques of its parameters control.

1 INTRODUCTION

The electron cooling, suggested by G.I.Budker in 1967 [1], is based on the interaction of heavy hot particles with a cold electron beam. In the forthcoming experiments in Novosibirsk feasibility of realizing this idea was shown and peculiarities of a cooling process were discovered [2]. The electron cooler for the heavy ions synchrotron at GSI is one of the devices successfully working in accelerators [3]. The main part of the cooler is a large solenoid with a high uniformity of magnetic field, so, it's worthwhile to describe the experience in building such a device and in methods of its parameters control.

2 GENERAL DESCRIPTION OF THE ELECTRON COOLER

The electron cooler (Fig. 1) consists of the following parts:
a) a magnetic system that forms and transports the electron beam from the gun to the collector;
b) an electron gun and the collector;
c) a vacuum chamber with pumping equipment.

The magnetic system consists of a main precision solenoid with a uniform magnetic field; of two toroids of 45 degrees turns; of two short solenoids, adjoining the toroids and two short solenoids of the gun and the collector.

3 PRECISION SOLENOID

3.1 Choice of parameters

Following the GSI ions synchrotron parameters: beam dimensions in a free straight section equal to about 20 cm (3σ) and the time of cooling of about 0.1 s [4] - the inner diameter of the solenoid was chosen to be 40 cm and the length of the uniform magnetic field region to be 3 m. The total mechanical length of the solenoid including the regions for the electron beam lead-in/lead-out to the ion trajectory was chosen to be 3.35 m.

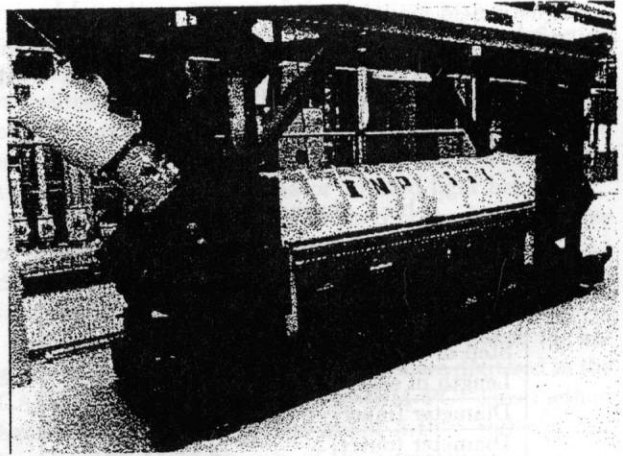


Figure 1: General view of the electron cooler

Let's determine the homogeneity of the magnetic field essential for cooling. The initial amplitude of the ion oscillation in the cooler is about $a=4$ cm and the final one should be about 0.1-0.2 cm. During the particle motion through the cooling section with a β -function β and length L ions deviate in the transverse direction of about aL/β . For an effective cooling the deviation angle due to the transverse component of the magnetic field α should be less than an ion beam angle, e.g. a/β . For $a=0.1-0.2$ cm and $\beta = 12$ m it follows that $H_{\perp}/H < 10^{-4}$.

The solenoid consists of 58 short coils connected in series to a current power supply and connected in parallel to cooling water. The coils are wound with a copper busbar of a cross-section $7 \times 7 \text{ mm}^2$. The coil size: the inside diameter is 40 cm, the outer diameter is 52 cm, the length is 5.8 cm, the number of turns is 6×6 , the coil current at the magnetic field of 1500 G does not exceed 200 A.

Let's consider the requirements to the precision of the solenoid coil manufacturing.

An integration along the current conductor is used to calculate the solenoid field. Transitions from one layer to the other create transverse fields at the solenoid axis. The result of calculations shows that the maximum transverse magnetic field along the coil axis at a 200 A current is equal to 0.15 G. However, a large coil radius of 20 cm gives a weak field dependence along the axis. As a result, if we sum up the fields of all the coils, the transverse field modulations along the solenoid decrease substantially due to mutual compensation. The transverse field alters peri-

odically with a coil step λ by 0.001 G, and the longitudinal field modulation with a 7 cm step alters by 0.03 G. In this case, due to this modulation at the radius r the transverse field can be found according to the formula:

$$B_r = \frac{r}{2} \cdot \frac{dB_z}{dz} = \frac{\pi \Delta B_z r}{\lambda}, \quad (1)$$

being equal to 0.05 G at a 4 cm radius, i.e., the relative magnetic field modulation is 4×10^{-5} .

So, if the accuracy of the turn position is about 0.5 mm, we can achieve a field parallelism better than $7 \cdot 10^{-5}$ without extra field correctors.

Other parameters of the solenoid are listed in Table 1.

Table 1. Solenoid parameters

Magnetic field	400 -1500 G
Number of layers	6
Number of turns in a layer	335
Step of winding	1.00 cm
Length of solenoid	335.00 cm
Diameter (inner)	40.00 cm
Diameter (outer)	52.00 cm
Resistance	1.68761 Ohm
Mass of copper	860.66 kg
Mass of insulation	579.01 kg
Mass of iron	430.70 kg
Thickness of iron shield	1.00 cm
Current for H=1500 G	198.94 A
Voltage	335.74 V
Power	66.79 kW

3.2 Manufacturing coils and solenoid

According to capability of the Pilot Production Plant at BINP we decided to make the solenoid assembled of separate coils. It minimises the influence of the current leads on the magnetic field homogeneity and decreases the value of the current supplied. Moreover in the case of a multiturn coil the influence of the turns displacement is significantly smaller due to mutual subtraction.

The basis of the solenoid is a frame 1 and a prism 2 (Fig.2), forming a rigid support of the installation. The prism 2 together with a cover 3 forms the magnetic flux return.

The coils of the solenoid were mounted on a plane E of aluminium alloy supporting bars. Surfaces E and surfaces F were treated with high accuracy for one operation: the nonflatness of E and F surfaces along the whole length of about 3.5 m was no worse than 0.05 mm. At the one end of the aluminium bars a plate was rigidly fixed perpendicularly to the surfaces E and F. The coils were nestled to this plate and subtended to a monolithic package with the four pins H and with the other mobile plate at the opposite end of the bars. The gaps between the surface E and the supports 8 of the coils (Fig.3) were less than 0.03 mm. Surfaces F allow to inspect the position of the plates after

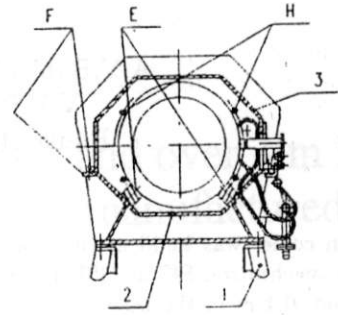


Figure 2: Cross section of the solenoid

the assembly of a the solenoid, and serve as a bindings of the cooler to the synchrotron.

The coils (Fig. 3) were wound with a square copper bus, 7x7 mm in cross section with a bore 4 mm in diameter. The bus was covered with two layers of mylar and a glass tape insulation.

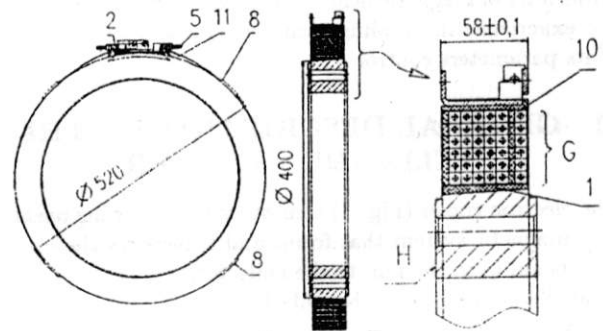


Figure 3: Solenoid coil

The coils were wound in two stages: at first - six layers of 30 turns in one direction and then - 6 turns G in the form of Archimed spiral in the opposite direction. Spacers 10 made of an insulation material, strictly fixed at winding of a coil, provide smooth transition of the bus from one layer to another and precise fixation of the bus inside coils.

The basic technological element for the coil manufacturing was a rigid precise steel ring H, at which all main operations were performed.

At the beginning a moulded G-10 shell 1 was processed coaxially with the ring H. Then the ring was installed to the fixture at the winding machine and winding was completed. After that the power supply contacts 2 with water connectors 5 were soldered to the bus; spacers 11 and sup-

ports 8 were installed; all that was wrapped with a glass tape and filled with the epoxy compound. When the epoxy compound became hard the processing of the coil support 8 coaxially with the ring H was done with an accuracy of about 0.07 mm. Then the ring H was removed and after that the support 8 became the basic element for installing the coil to the solenoid.

Each coil manufactured was tested to determine the direction of its magnetic field force line with respect to the coil surface. For this purpose two coils with opposite magnetic fields were placed with a gap of about 1 cm coaxially one over the other. The surfaces of the coils were adjusted in parallel with an accuracy better than $2 \cdot 10^{-4}$. The lower coil was fixed, but the upper coil could be rotated around the axis. At the same axis, in the centre between the coils a Hall probe was placed to measure the transversal component of the coil magnetic field. So, if the magnetic field of the upper tested coil is not perpendicular to its surface, the Hall probe signal is sinusoidal (see, the upper curve in Fig.4).

The amplitude and phase of the Hall probe signal determine the angle and azimuth of the inclination of the coil. All the coils with a field inclination angle over 10^{-4} were additionally processed to eliminate the inclination. The procedure was repeated as many times as the angle between the magnetic field and perpendicular to the coil surface decreased below 10^{-4} .

Fig.4 presents the magnetic field measurements before (upper curve) and after (lower curve) the additional processing of one of the coils.

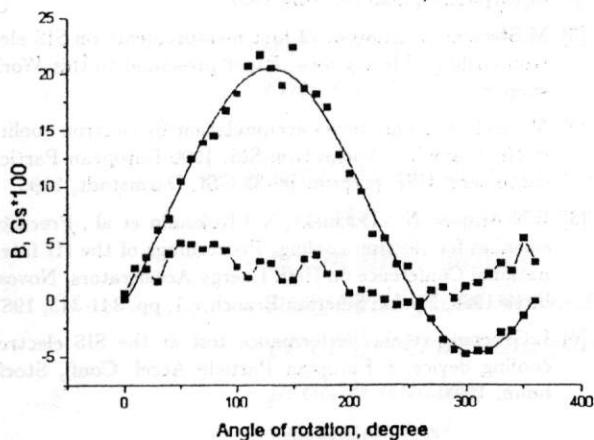


Figure 4: Transverse magnetic field of the coil vs. the angle of rotation.

4 MAGNETIC FIELD MEASUREMENT IN THE SOLENOID

4.1 Techniques of field measurements

We used two methods to control the magnetic field homogeneity in the solenoid.

In the first one [5] magnetic field homogeneity is determined from the readings of the direction of the magnetic compass moved along the solenoid axis. The deflection of the compass needle axis during the mirror movement is measured optically with the help of a small mirror mounted on the compass and autocollimator of AF-1Tz, detecting an angle between the falling onto and the reflected from the mirror of an autocollimator infrared light beam.

A great advantage of this method is the independence of the rail quality (deflections, ledges at joint points, etc.) during the mirror movement because the compass needle is always directed along the magnetic field force line.

Signals from the autocollimator proportional to the angle in the horizontal and vertical planes are digitized in the CAMAC module and directed to IBM PC. This method has an accuracy in angles of about $5 \cdot 10^{-6}$ rad and due to a limited dynamic range of the autocollimator can be used in the magnetic field with homogeneity better than $1.5 \cdot 10^{-3}$.

The second method based on a general Hall probe technique was used to measure magnetic fields in all parts of the cooler: in the toroids, in the gun and collector solenoids and, as a control, in the main solenoid. We used commercial GaAs detectors $1.5 \times 1 \times 0.1 \text{ mm}^3$ in size connected in series with 100 mA stable (0.001 mA) current power supply. Their signals were digitized by a CAMAC voltmeter and transmitted to the IBM PC.

All Hall probes were glued to sides of a copper $5 \times 5 \times 3 \text{ cm}^3$ parallelepiped which could be moved on the same rail as the mirror for optical field measurements. The parallelepiped was installed on the rail in such a way that the central (axial) detector was placed on the solenoid axis with a larger surface normal to the axial field. The other four detectors were glued to the centres of lateral sides. They were intended for the measurement of transverse fields.

Before the measurement all Hall detectors was calibrated in the uniform field of a test dipole with the help of NMR probe in the range from 300 up to 1500 G. The calibration allows to determine the sensitivity of each Hall probe to the normal and parallel to the probe's surface components of the field. This data were used in the treatment of the field measurements.

4.2 Results of measurements

The main goal of the magnetic measurements was to measure the field geometry in the cooling section to calculate required corrections in the coil positions compensating for non-homogeneity of the magnetic field. Another purpose was to measure the magnetic field of the coils intended

for changing the electron beam position and to measure magnetic fields along the ion beam trajectory necessary for calculating the influence of the cooler magnetic field on the ion movement in the synchrotron.

Fig. 5 shows the distribution of the magnetic field that accompanies the electron beam from the gun to the collector at a 600 G magnetic field in the main solenoid.

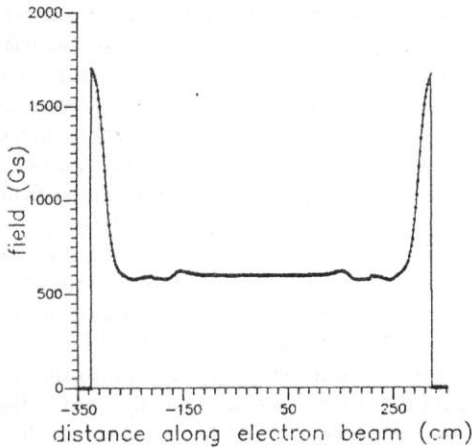


Figure 5: Magnetic field along the electron trajectory

Fig. 6 presents the vertical component of the field in the solenoid. As it's seen the transverse component of the magnetic field in the solenoid is quite large and an additional correction of the field is needed.

We used a coil inclination method to make the solenoid magnetic field more uniform.

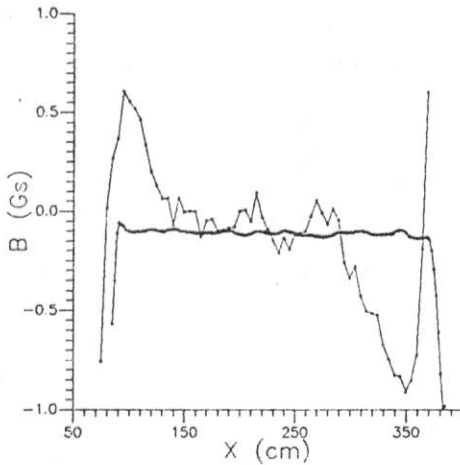


Figure 6: Transverse component of the magnetic field in the solenoid before corrections and calculated one after an appropriate inclination of the coils

4.3 Solenoid field correction by coils inclination

If the axis of the coil is inclined to the solenoid axis, then a transverse magnetic field appears proportional to the

inclination angle. A program code for an automatic selection of the angles for the transverse fields correction in the solenoid was written to select the inclination amplitude. It helps to select the spacers between the coils to correct magnetic field distribution.

The result of the vertical field component correction by this method is presented in Fig.6.

As it is seen the vertical component of the magnetic field over a length of about 3m is better than 0.05 G at 1500 G of the main field component.

The magnetic field measurements made at GSI [6] showed that the uniformity of the magnetic field was about 10^{-5} .

5 CONCLUSION

The precise solenoid about 3 m long and 0.4 m in the inner diameter, with a magnetic field homogeneity of approximately 10^{-5} was created for the electron cooling device at GSI, Darmstadt. The first experiments to cool ion beams at the GSI synchrotron showed high quality of the magnetic field in the cooler.

6 ACKNOWLEDGEMENTS

Many thanks to Dr.Boris Baklakov and Alexandr Erokhin for designing of a stable low noise amplifier for Hall probes, which allows us to measure magnetic fields as low as 0.01-0.05 G. The authors express their gratitude to Mrs.Lena Lisman for reading and correcting this article.

7 REFERENCES

- [1] G.I.Budker, Efficient method for damping of particle oscillations in proton and antiproton storage ring. *Atomnaya Energiya* 22,346-8,1967.
- [2] V.V.Parkhomchuk and A.N.Skrinsky, Electron cooling: physics and prospective applications. *Reports on Progress in Physics*,v.54,num.7, July 1991.
- [3] M.Steck et al, Analysis of first measurements on SIS electron cooling of heavy ions, Paper presented to this Workshop.
- [4] M.Steck et al, Fast beam accumulation by electron cooling in the heavy ion synchrotron SIS, 1996 European Particle conference, GSI- preprint 96-33,GSI, Darmstadt, 1996.
- [5] L.N.Arapov, N.S.Dikansky, V.I.Kokoulin et al., Precision solenoid for electron cooling. *Proceedings of the III International Conference on High Energy Accelerators*, Novosibirsk 1986, Nauka, Siberian Branch,v.1, pp. 341-343, 1987.
- [6] L.Groening et al., Performance test at the SIS electron cooling device, 6 European Particle Accel. Conf., Stockholm, 1998.